BIOCHEMISTRY
including biophysical chemistry & molecular biology

Article

pubs.acs.org/biochemistry

Protein Dynamics Are Influenced by the Order of Ligand Binding to an Antibiotic Resistance Enzyme

Adrianne L. Norris,[†] Jonathan Nickels,[‡,§] Alexei P. Sokolov,*[,‡,§] and Engin H. Serpersu*[,†,∥]

[†]Department of Biochemistry and Cellular and Molecular Biology, The University of Tennessee, Knoxville, Tennessee 37996, United States

[‡]The Joint Institute for Neutron Sciences, Oak Ridge National Laboratory, Knoxville, Tennessee 37831-6453, United States

[§]Department of Chemistry, The University of Tennessee, Knoxville, Tennessee 37996, United States

[∥]Graduate School of Genome Science and Technology, The University of Tennessee and Oak Ridge National Laboratory, Knoxville, Tennessee 37996, United States

S *Supporting Information*

ABSTRACT: The aminoglycoside N3 acetyltransferase-IIIb (AAC) is responsible for conferring bacterial resistance to a variety of aminoglycoside antibiotics. Nuclear magnetic resonance spectroscopy and dynamic light scattering analyses revealed a surprising result; the dynamics of the ternary complex between AAC and its two ligands, an antibiotic and coenzyme A, are dependent upon the order in which the ligands are bound. Additionally, two structurally similar aminoglycosides, neomycin and paromomycin, induce strikingly different dynamic properties when they are in their ternary complexes. To the best of our knowledge, this is the first example of a system in which two identically productive pathways of forming a simple ternary complex yield significant differences in dynamic properties. These observations emphasize the importance of the sequence of events in achieving optimal protein−ligand interactions and demonstrate that even a minor difference in molecular structure can have a profound effect on biochemical processes.

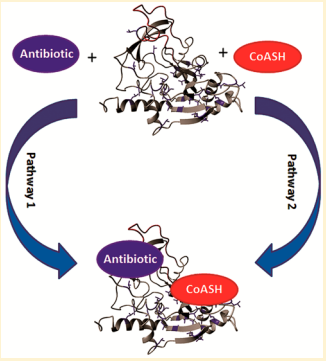

Aminoglycoside antibiotics make up a large group of antibiotics produced by actinomycetes as a defensive measure against other bacteria,[1−3] where they bind to 16S RNA of the 30S ribosome and interfere with protein synthesis, eventually causing cell death.[4,5] Although there are multiple modes of resistance to their action, the principal mode of resistance is the enzymatic modification of these antibiotics via N-acetylation, O-nucleotidylation, or O-phosphorylation by a large number of aminoglycoside-modifying enzymes (AGMEs) known today.[1,3,6−8] These enzymes show different levels of substrate promiscuity, and a given enzyme can modify several structurally diverse aminoglycosides. However, the molecular basis of their substrate promiscuity remains largely unexplained. In this paper, we describe the unusual properties of one of these enzymes, aminoglycoside N3 acetyltransferase-IIIb (AAC). Our findings highlight the role of protein dynamics in substrate promiscuity. Specifically, we demonstrate how the dynamics of the enzyme are changed by even the smallest differences between structurally similar ligands and that these changes have measurable consequences. Moreover, our results reveal that the order of ligand binding during the formation of ternary complexes does make a difference in the dynamics of the complex.

From binding studies, it has been shown that the apo form of AAC can associate with either coenzyme A alone (AAC−CoASH complex) or the antibiotic alone (AAC−antibiotic complex) with micromolar or higher affinity.[9,10] Formation of the ternary complex by addition of aminoglycoside (AG) to the binary AAC−CoASH complex is accompanied by an increase in antibiotic affinity of 5−20-fold.[9] Conversely, addition of CoASH to a binary AAC−AG complex does not alter CoASH affinity.[10] Ternary complex formation is enthalpically more favored and entropically more disfavored than those of either binary complexes. Data presented in this paper demonstrate that the dynamics of a ternary complex formed by different pathways might or might not be identical despite the fact that the total overall enthalpy of ternary complex formation is independent of pathway and Hess' law is obeyed.[9]

These data strongly suggest that association of CoASH with AAC induces a conformational change that allows for optimal aminoglycoside interaction. Consequently, one wonders whether the formation of the ternary complex by addition of CoASH before AG leads to an AAC conformation different from that formed it in the reverse fashion by addition of AG before CoASH. Experimental results presented here provide support for the hypothesis that the order of addition of substrate to AAC does indeed make a difference and yields ternary complexes with different dynamic properties. We emphasize that both pathways of ternary complex formation show the same kinetic parameters (Figure S1 of the Supporting

Received: March 11, 2013
Revised: December 9, 2013
Published: December 9, 2013

   dx.doi.org/10.1021/bi401635r | *Biochemistry* 2014, 53, 30−38

Information) so the observed differences are not due to the formation of a dead-end complex.

MATERIALS AND METHODS

Chemicals and Reagents. Deuterium oxide (D_2O) (99.9%), ^{15}N-enriched salts (99%), and ^{15}N-labeled amino acids (≥98%) were purchased from Cambridge Isotope Laboratories (Andover, MA). Aminoglycoside antibiotics, coenzyme A, and all other chemicals and reagents were purchased at the highest purity available from Sigma-Aldrich.

Overexpression and Purification of AAC. AAC was overexpressed by addition of 1 mM isopropyl thiogalactopyranoside (IPTG) to *Escherichia coli* BL21(DE3) cells grown to an optical density of ∼1.0 at 600 nm in either Luria Broth (for DSC experiments), M9 minimal medium containing $^{15}NH_4Cl$ (for uniform labeling of AAC with ^{15}N), or M9 minimal medium with a selected amino acids enriched with ^{15}N, while the remaining amino acids were unlabeled and individually added to the growth medium. All cells were grown and induced at 37 °C. Cells were harvested by centrifugation 4 h after induction with IPTG. In all cases, the AAC protein was isolated via nickel affinity chromatography followed by proteolytic removal of the six-His tag and a final purification to remove free six-His tag and thrombin as described previously.[9]

Ternary Complex Sample Preparation. Regardless of the experimental method, ternary complexes were formed in the same general fashion. First, to a solution containing the method appropriate concentration of AAC was added the first ligand from a concentrated stock to the desired concentration, and the solution was gently mixed. This complex was allowed to incubate at 25 °C for 10 min. Longer incubation periods did not change experimental results. Finally, the second ligand was added to the solution from a concentrated stock in the same manner. With each method, all samples were identically prepared to minimize preparation errors and experiments promptly performed. All ligand concentrations were calculated on the basis of previously determined dissociation constants.[9,10] To simplify the description, the ternary complexes are written in the order in which the substrates were added to AAC based on the two possible pathways of ternary complex formation (Figure 1).

Pathway 1:

AAC + Neomycin ⇌ AAC-Neomycin + CoASH ⇌ AAC-Neomycin-CoASH

Pathway 2:

AAC + CoASH ⇌ AAC-CoASH + Neomycin ⇌ AAC-CoASH-Neomycin

Figure 1. Two possible pathways of ternary complex formation.

Nuclear Magnetic Resonance (NMR). All NMR spectra were recorded by a Varian Inova 600 MHz triple-resonance spectrometer equipped with a ^{1}H, ^{13}C, ^{15}N triple-resonance cryogenic probe at The University of Tennessee. Sensitivity-enhanced $^{15}N-^{1}H$ heteronuclear single-quantum coherence (HSQC)[11] experiments with the *TROSY* option[12] were performed with either uniformly labeled [^{15}N]AAC or [^{15}N]leucine-labeled AAC at concentrations of 150−230 μM in 50 mM MOPS [3-(*N*-morpholino)propanesulfonic acid] buffer and 100 mM NaCl (pH 7.6) at 29 °C. Spectra were recorded with 24−64 scans of 64 increments in the ^{15}N dimension and a delay of 1.5 s between scans; 2048 data points were collected with an acquisition time of 128 ms. Hydrogen−deuterium exchange was followed for >90 h by successive acquisition of $^{1}H-^{15}N$ correlation spectra in samples immediately after they had been dissolved in D_2O. Solvent-exposed amide (SEA)[13,14] HSQC spectra were taken at mixing times of 5−200 ms. After data had been collected, enzyme activity was kept at >80% of that measured before experiments. As a further check of enzyme integrity, a normal HSQC spectrum was taken before and after each experiment, and no changes were observed because of either the experimentation time or the lyophilization process. NOESY-HSQC spectra[11,15] were recorded with the two ternary complexes of enzyme, CoASH, and neomycin, prepared by reversing the order of addition of the ligand to the enzyme as described above (Figure 1). In both cases, the concentration of [^{15}N]AAC was matched at 170 μM in a 320 μL volume in Shigemi tubes, and both substrates were added in sufficient quantity to render >98% of the enzyme in the ternary complex. Data were acquired using eight scans with 128 increments in the proton dimension and 48 increments in the nitrogen dimension; 1440 data points with an acquisition time of 85 ms were collected on a spectral window of 8446 Hz in the proton dimension.

Data were processed with NMRpipe,[16] where the FID was multiplied with a $\sin^2$ window function in the acquisition dimension before Fourier transformation. No baseline correction or other cosmetic procedures were applied. Two-dimensional (2D) spectra were exported to Sparky (T. D. Goddard and D. G. Kneller, *SPARKY 3*, University of California, San Francisco) for analysis and display. Three-dimensional NOESY-HSQC spectra were displayed and analyzed by nmrview.[17]

Differential Scanning Calorimetry (DSC). DSC experiments were performed on a VP-DSC microcalorimeter from MicroCal. Melting transition data were collected between 25 and 70 °C and analyzed with Origin software using a non-two-state model for fitting of DSC curves. Because heat denaturation was found to be irreversible as cooling and subsequent reheating yielded dissimilar traces of unfolding, even when the stopping temperature of the DSC scan was set to directly after the observed T_m, data could not be reliably fit to determine ΔC_p.[18,19] Therefore, all interpretation of data is limited to the melting temperature. All samples contained 30 μM AAC in 50 mM MOPS and 100 mM NaCl (pH 7.6). An identical solution without protein and/or ligands was used in the reference cell. The change in ligand saturation due to the increasing temperature in the DSC experiment was calculated to be ≤10% based on known temperature dependencies of the dissociation constants for each ligand. As a control, experiments were performed under identical conditions at various protein concentrations between 20 and 60 μM to ascertain any effect of artificial oligomerization. No effect was observed. All samples were degassed for 5 min prior to being loaded.

Dynamic Light Scattering (DLS). AAC samples were prepared in 50 mM MOPS (pH 7.6) and 100 mM NaCl to a concentration of 1 mg/mL. The protein was airfuged for 1 h and the top 75% of the supernatant used for DLS experiments. Where appropriate, CoASH and antibiotics were present at concentrations sufficiently high to saturate 95% of the protein binding sites and complexes prepared as described above. Experiments were performed within 24 h of sample preparation. Directly before scattering experiments, samples were centrifuged, and the supernatant was subsequently filtered with a 0.2 μm filter into optical cuvettes for measurement. Dynamic light scattering was measured at 20 °C in a backscattering geometry using a Lexel-95 Kr ion laser with a

dx.doi.org/10.1021/bi401635r | *Biochemistry* 2014, 53, 30−38

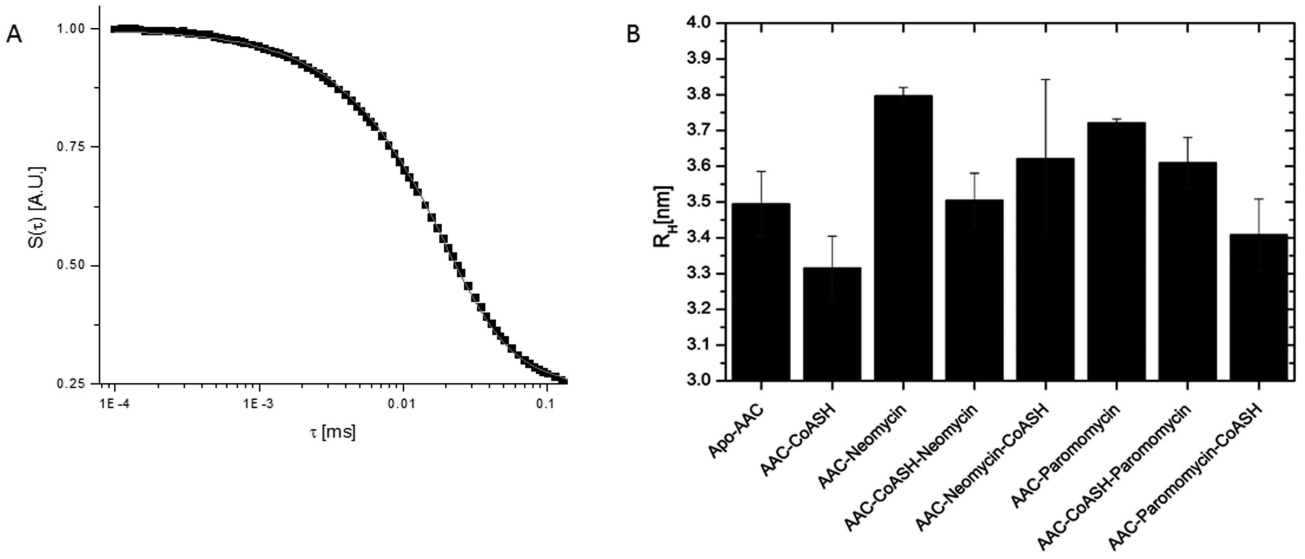

Figure 2. (A) DLS data for apo-AAC (■) and their fit (—). The exponential fit provides an estimate of the decay rate Γ that is directly related to the hydrodynamic radius of the protein or its complex. (B) Hydrodynamic radii of AAC and its complexes are dependent on the pathway and antibiotic. Hydrodynamic radii (R_H) are shown in nanometers for apo-AAC and binary and ternary complexes with neomycin, paromomycin, and coenzyme A. The statistical significance of the observed differences is presented in Table S1 of the Supporting Information.

wavelength λ of 647.1 nm and a power of ~30 mW. Scattered light was collected with a single-mode optical fiber. Then the light was split into two Avalanche photodiodes and cross correlated via an ALV-7004/Fast digital correlator. To achieve good statistics, each sample was measured six times. From the six obtained values, the smallest and the largest were discarded, and the averaged value and standard deviations were calculated using the four remaining values.

Dynamic light scattering measures the intensity−intensity correlation function

$$\varphi\, |g_1(t)|^2 = \frac{\langle I(0)I(t)\rangle}{\langle I\rangle^2} - 1$$

where $I(t)$ is the light scattering intensity. In diffusion, the autocorrelation function $\varphi(t)$ can be fit by the square of a single-exponential decay, $\varphi(t) = A\exp(-2\Gamma t) + C$, where decay constant $\Gamma = \mathbf{q}^2 D$. Here D is a diffusion coefficient, and $\mathbf{q}$ is the scattering wavevector that for the backscattering geometry and the refractive index of our solution ($n_0 = 1.33$) is $\mathbf{q} = (4\pi n_o/\lambda) = 0.0258\ \text{nm}^{-1}$. The diffusion coefficient allows direct estimates of the hydrodynamic radius of the molecule through the Stokes−Einstein relation, $R_H = (kT)/(6\pi\eta D)$, where k is the Boltzmann constant, T (293 K) is the temperature of the measurements, and η (1 mPa/s) is the solvent viscosity.

Analytical Ultracentrifugation. All sedimentation velocity (SV) experiments were performed in a Beckman XL-I analytical ultracentrifuge. Prior to centrifugation, the protein was dialyzed into 50 mM MOPS (pH 7.6) and 100 mM NaCl, and the resulting dialysate was used as a reference. After the addition of CoASH and/or aminoglycoside, 400 μL samples were placed in double-sector cells. Samples were equilibrated for 2 h under vacuum at 25 °C and then run for 8 h at 50000 rpm. Sedimentation of AAC was monitored by the absorbance at 280 nm. Sedimentation coefficients were determined by $c(s)$ analysis using SEDFIT.[20,21] Size distribution analysis of macromolecules was conducted by sedimentation velocity ultracentrifugation and Lamm equation modeling.[20]

RESULTS

The AAC−CoASH−Neomycin Complex Is Not Identical to the AAC−Neomycin−CoASH Complex. To test the hypothesis that two pathways of ternary complex formation result in nonequivalent protein dynamics, DLS experiments were performed to estimate the hydrodynamic radius of the protein in its binary and ternary complexes. Examples of raw data are shown in Figure 2A, where data points with an exponential fit that provides an estimate of the decay rate constant Γ that allows determination of the hydrodynamic radius of the complex as described in Materials and Methods are depicted. The hydrodynamic radius represents the average size of the diffusing complex. Figure 2B shows the hydrodynamic radii for apo-AAC and its binary and ternary complexes. Here, apo-AAC was found to have a hydrodynamic radius (R_H) of ~3.5 nm. Analytical ultracentrifugation demonstrates that AAC in solution exists as a dimer with a total molecular mass of ~58 kDa both with and without ligands and is independent of the order of substrate addition. Therefore, the obtained R_H is reasonable for a molecule of this size.[22]

Comparison of the hydrodynamic radius upon complex formation clearly shows that the binding of the antibiotic or CoASH induces changes in the hydrodynamic radius of AAC (Figure 2B). The size of the protein decreases slightly upon binding of CoASH. Moreover, the hydrodynamic radius of ternary complexes appears to be smaller than those of binary (enzyme−antibiotic) complexes. Most interesting and unexpected is the observation that the R_H of the ternary complex depends on the order in which it was formed. The larger radius for the AAC−neomycin−CoASH complex relative to that of the AAC−CoASH−neomycin complex suggests that the addition of neomycin first does result in a ternary complex with less compact structure. The opposite behavior is observed for ternary complexes with paromomycin (Figure 2B), in which binding of the antibiotic first leads to formation of the more compact structure. Neomycin and paromomycin are different only in the 6′ functional group (Figure S2 of the Supporting

dx.doi.org/10.1021/bi401635r | Biochemistry 2014, 53, 30−38

Information) yet hold a strongly differential influence over the protein's dynamics. We notice comparatively large error bars, especially for the ACC−Neo−CoASH complex, and performed analysis of the statistical significance for the observed differences in R_H (Figure 2B). The analysis shows statistically significant difference for most of the samples (see Table S1 of the Supporting Information, as computed by a two-tail t test assuming unequal variance for each combination of samples).[23] This emphasizes the incredible substrate recognition capabilities of AAC.

As the DLS data suggested that there is an observable difference in the hydrodynamic radius of the protein as a whole, ^{15}N−^{1}H HSQC data were acquired with uniformly ^{15}N-labeled AAC to probe the order of ternary complex formation at an amino acid level. The ^{15}N−^{1}H spectrum of AAC is well dispersed for a 58 kDa protein in which chemical shifts as a result of ligand binding can be followed for many resonances.[10] In one experiment, AG was titrated to AAC followed by titration of CoASH, with HSQC spectra obtained after each titration point. The reverse titration was also performed in which CoASH was titrated first and then AG. Considering only the well-resolved peaks, five peaks in the spectrum of the AAC−neomycin−CoASH complex displayed line widths significantly broader than those of the spectrum of the AAC−CoASH−neomycin complex. Table 1 lists data for three such peaks (1−3) and three other peaks (4−6) that do not undergo significant changes and serve as internal controls. Overall, as the line widths of the well-resolved signals and not their chemical shifts are affected, these data suggest that several regions of the protein backbone show different dynamic properties in the final conformations of the two ternary complexes. Thus, these phenomena appear to be related to protein motion and not differential ternary complex structures.

Table 1. Properties of Selected Resonances Behaving Differentially in Ternary Complexes[a]

complex	peak	^{15}N (ppm)	^{1}H (ppm)	height	^{1}H lw$_{1/2}$ (Hz)	^{15}N lw$_{1/2}$ (Hz)
AAC−CoASH−neomycin	1	108.2	7.09	7883	65.0	34.8
AAC−neomycin−CoASH				9241	50.0	25.7
AAC−CoASH−neomycin	2	114.4	9.08	6559	52.1	24.5
AAC−neomycin−CoASH				9374	38.4	34.5
AAC−CoASH−neomycin	3	131.3	8.55	7262	45.9	36.2
AAC−neomycin−CoASH				9270	61.1	24.3
AAC−CoASH−neomycin	4	107.7	7.25	15937	48.7	31.7
AAC−neomycin−CoASH				15925	42.4	25.2
AAC−CoASH−neomycin	5	117.0	9.13	15223	40.6	39.7
AAC−neomycin−CoASH				16610	42.0	34.8
AAC−CoASH−neomycin	6	128.7	9.00	17284	34.9	24.4
AAC−neomycin−CoASH				16918	36.3	27.0

[a]Peaks 1−3 demonstrate significantly different peak heights and linewidths upon formation of ternary complexes. Peaks 4-6 serve as controls that do not show such behavior and are in comparable regions of the spectrum as peaks 1-3.

To probe whether there is an observable interconversion between the two ternary complexes, NMR spectra were acquired over several days. No changes in the positions and intensities of those peaks that were different between the HSQC spectra of two complexes were detected. Thus, any interconversion between the two ternary complexes is very slow, or the thermodynamic barrier between them is too high. Longer experiments could not be interpreted because of the instability of the protein over extended periods of time.

To simplify the spectra, AAC protein enriched with only [^{15}N]leucine was produced. Here, differences between the ternary complexes become quite prominent. In the absence of any ligand, the HSQC spectrum shows ∼27−28 of a possible 29 leucine peaks. This coincides well with the protein structure as there is one leucine residue in the middle of the antibiotic binding loop and none within 10 residues of the flexible N- or C-terminus (Figure S3 of the Supporting Information).[9,24] Amino acids in such flexible regions often demonstrate line broadening as a result of conformational sampling on an intermediary exchange time scale.

The [^{15}N]leucine spectrum for the AAC−neomycin−CoASH complex shows several peaks that cannot be superimposed with those of the spectrum of the AAC−CoASH−neomycin complex (Figure 3a). Specifically, a clustering of

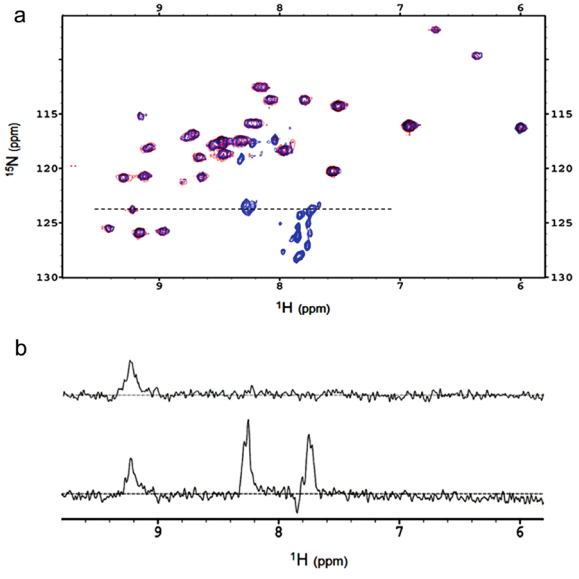

Figure 3. NMR spectra of pathway 1 and pathway 2 are not identical. (a) Superimposed spectrum of the [^{15}N]leucine-labeled AAC−CoASH−neomycin complex (red) and the AAC−neomycin−CoASH complex (blue) taken at identical contour levels. Most peaks are completely superimposable and appear purple. (b) ^{1}H dimension slice at the dashed line of panel a. The top trace in panel b is that of the AAC−CoASH−neomycin complex and the bottom trace that of the AAC−neomycin−CoASH complex.

peaks as observed between 7.6 and 8.4 ppm for the AAC−neomycin−CoASH complex is absent in the AAC−CoASH−neomycin complex. This type of clustering is usually observed when an amide is in a segment of the backbone that has multiple structural conformations with slow interconversion rates. To ascertain that this pattern is not due to any type of protein degradation, we performed MS analysis on both ternary

dx.doi.org/10.1021/bi401635r | Biochemistry 2014, 53, 30−38

complexes. Results shown in Figure S4 of the Supporting Information confirmed that both complexes are intact. Thus, certain region(s) of AAC that contain leucine residues are flexible and can fluctuate between conformations. The originally missing resonance located in the antibiotic binding loop is one candidate for this. However, the number of peaks in this region suggests that several other leucines may also be fluctuating slowly between multiple conformational states in this complex. As there are no hints of resonances in this area for the AAC−CoASH−neomycin complex (Figure 3b) and all the visible peaks in both spectra are perfectly superimposed, these data indicate that the dynamics of several segments of the protein backbone are significantly different in the ternary complexes. In other words, the AAC−CoASH−neomycin complex appears to be less dynamic (or more well-defined) than the AAC−neomycin−CoASH complex.

Differences between the two ternary complexes were also observed in NOESY-HSQC experiments. Figure 4 shows ^{1}H−^{1}H NOESY patterns on several 2D planes taken at different ^{15}N chemical shifts. Consistent with the observations described above, the AAC−CoASH−neomycin ternary complex shows additional NOE cross-peaks compared to those observed with the AAC−neomycin−CoASH ternary complex, indicating that the dynamic properties of both complexes are different. As shown in Figure 4, differences in NOE patterns of the peaks that overlap in both spectra are not limited to certain parts of the protein but are visible between backbone amides or between amides and CαH groups as well as amides and side chain protons. In all cases, the spectrum of the AAC−CoASH−neomycin complex shows more NOEs than the spectrum of the AAC−neomycin−CoASH complex, suggesting that it is the less dynamic of the two complexes.

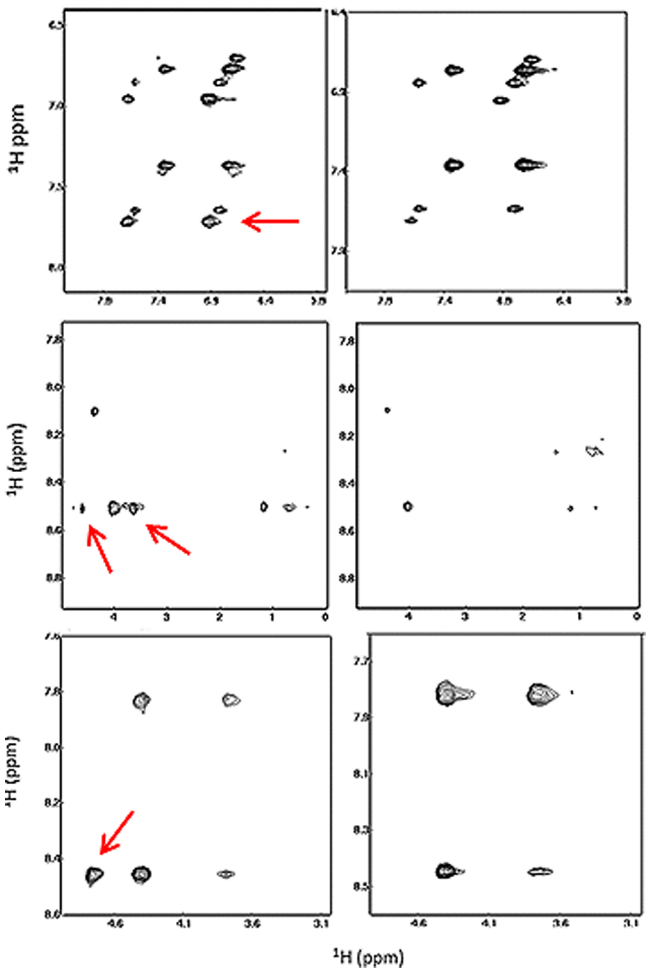

Figure 4. ^{1}H−^{1}H NOE peaks shown in ^{15}N planes at 112.6 ppm (top), 117 ppm (middle), and 118.8 ppm (bottom) for AAC−CoASH−neomycin (left) and AAC−neomycin−CoASH (right) complexes. NOEs observed only in the AAC−CoASH−neomycin complex are marked with arrows.

DSC experiments also demonstrated that the melting temperature is dependent on pathway. Here, the AAC−CoASH−neomycin complex has an upshift in its melting temperature (T_m = 50.1 ± 0.05 °C) relative to that of the AAC−neomycin−CoASH complex (T_m = 47.8 ± 0.03 °C) (Figure S5 of the Supporting Information). Moreover, the AAC−paromomycin−CoASH complex exhibits a melting temperature (45.5 ± 0.02 °C) higher than that of the AAC−CoASH−paromomycin complex (43.5 ± 0.02 °C), which is exactly the opposite of what was seen for the neomycin ternary complexes, thus paralleling the opposite trends observed in hydrodynamic radii. However, because DSC traces were not reversible, only qualitative conclusions could be drawn from these data and therefore serve only as support for the tendencies observed in NMR and DLS experiments.

We should note that the pathway-dependent effects observed in NMR and DLS experiments are not due to ligand-induced changes in the monomer−dimer equilibrium of the protein. Analytical ultracentrifugation studies with all complexes, as seen in Figure 5, show that the enzyme exists as a dimer in all complexes, and no traces of any other oligomeric forms are detected.

Ternary Complexes Also Demonstrate Differential Solvent Exposure. Various effects of solvent on ligand binding and protein folding has been described for different systems;[25−31] however, we previously observed a highly unique influence of aminoglycosides on the solvent structure at the protein−solvent interface.[9,32,33] Because the data discussed above illustrate that the AAC−neomycin−CoASH and AAC−CoASH−neomycin complexes have differential dynamic properties, it follows that the protein−solvent interactions may also be affected by the order of substrate addition.

To probe this possibility, the solvent-exposed amide (SEA) version of the ^{15}N−^{1}H HSQC experiment was utilized in which resonances appearing in the spectrum are only those that are exposed to solvent water.[13,14] Well-resolved peaks in the HSQC spectra of the AAC−neomycin−CoASH and AAC−CoASH−neomycin complexes show at least two resonances with differential behaviors (Figure 6). One is a strong peak present only in the AAC−CoASH−neomycin spectrum at 7.82 ppm (red). The second is weaker and situated at 7.94 ppm only in the AAC−neomycin−CoASH spectrum (blue). Although data shown in Figure 5 were collected with a mixing time of 100 ms, the observed differences begin to appear at mixing times as short as 5 ms; thus, NOE effects are not causing false positives. These resonances also cannot be artifacts of the SEA-HQSC experiment as both peaks are present in the regular ^{1}H−^{15}N HSQC spectrum for both ternary complexes. While we cannot yet identify these residues (resonance assignments are pending), it is clear that at least two amino acids have ternary complex-dependent solvent exposure.

A complementary set of NMR experiments were performed by direct measurement of hydrogen−deuterium exchange to investigate the potential for differential solvent−solute

dx.doi.org/10.1021/bi401635r | Biochemistry 2014, 53, 30−38

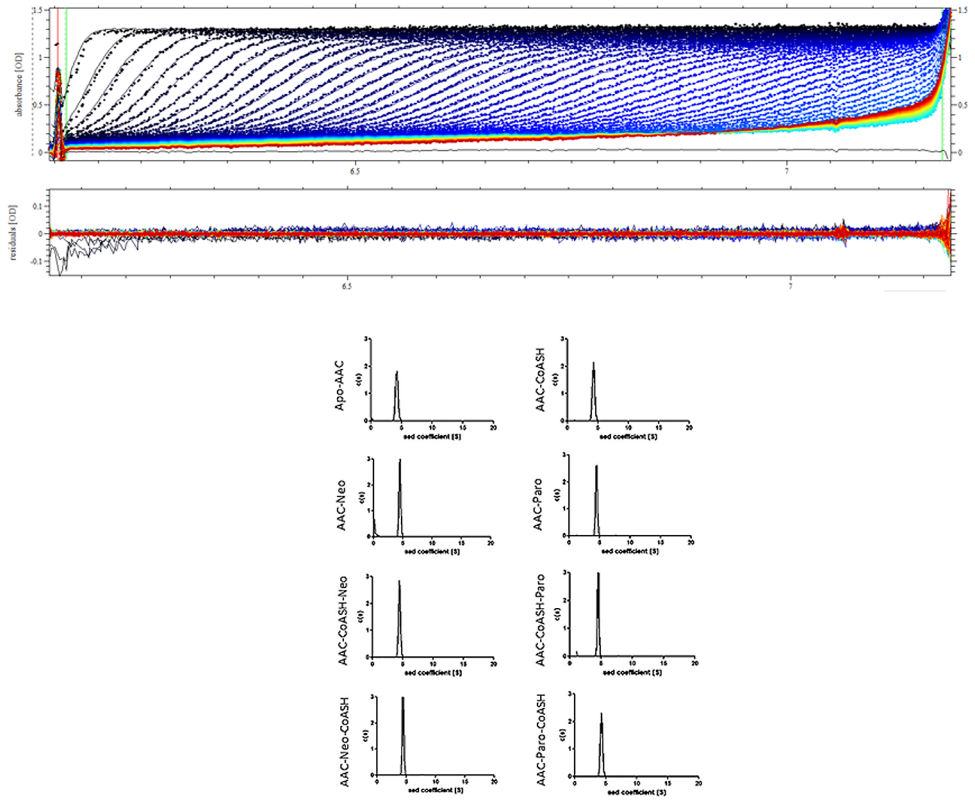

Figure 5. Determination of the molecular weights of apo-AAC and its ligand-bound complexes. Analytical ultracentrifugation representative raw data, acquired by analytical ultracentrifugation, are shown in the top panel, with sedimentation plots for all complexes shown in the bottom panel.

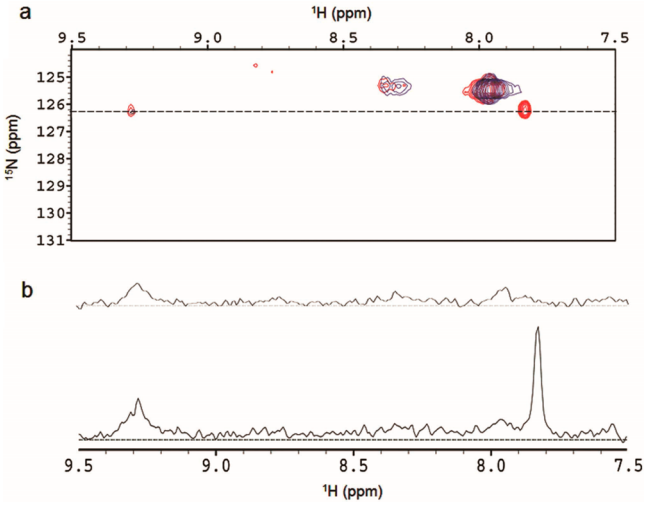

Figure 6. SEA-HSQC spectra of AAC−neomycin−CoASH and AAC−neomycin−CoASH complexes. (a) Superimposed spectra of AAC−neomycin−CoASH (blue) and AAC−CoASH−neomycin (red) complexes. The top portion of panel b is the one-dimensional ^{1}H slice of the AAC−neomycin−CoASH spectrum at the dashed line of panel a, while the bottom portion of panel b is that of the AAC−CoASH−neomycin spectrum. We note that these resonances are not localized to only one region of the spectrum and control peaks are in nearby regions. Also, because the changes in the crowded regions of the spectra could not be followed easily, they represent only a portion of the potential changes.

interactions in the two ternary complexes. Figure 7a illustrates that the HSQC spectra in the H_2O solvent (essentially time point zero of H−D exchange) of both ternary complexes are vastly superimposable, with only a few changes in peak intensities between the two as mentioned above. However, when solvent exchange occurred, differences in the intensity of several resonances between the two complexes became detectable as few as 5 min after exposure to D_2O where the vast majority of higher-intensity peaks belong to the AAC−CoASH−neomycin complex (Figure 7b). These differences become much more prominent at later time points (Figure 7c,d) and persist for >88 h after rehydration in D_2O, demonstrating stronger solvent protection consistently for the AAC−CoASH−neomycin complex. Thus, it is clear from both SEA and HD exchange experiments that there are regions of AAC that are less exposed to solvent when CoASH, and not neomycin, binds AAC first. This strongly supports the data from [^{15}N]leucine-labeled NMR and NOESY-HSQC spectra, which suggested that the AAC−CoASH−neomycin structure is less dynamic than the AAC−neomycin−CoASH structure. It also agrees well with the DLS data suggesting a more compact structure of the AAC−CoASH−neomycin complex.

DISCUSSION

In this work, we have demonstrated that the order of ligand addition significantly influences protein dynamics for AAC complexes as indicated by (1) changes in the hydrodynamic radii of the ternary complex as measured by DLS, (2) differential intensities of NOE patterns of peaks in NMR spectra of ternary complexes, and (3) differential solvent protection as detected by SEA and HD exchange NMR. In addition, a small difference in the structure of two antibiotics has a profound effect on ternary complexes with AAC and coenzyme A. The order of ternary complex formation has

dx.doi.org/10.1021/bi401635r | *Biochemistry* 2014, 53, 30−38

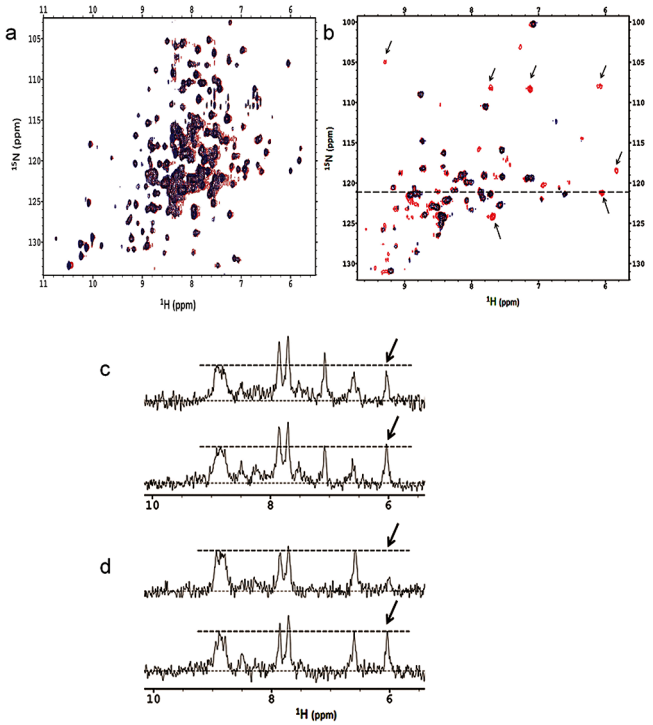

Figure 7. Solvent exposure patterns are different for pathway 1 and pathway 2. (a) Superimposed spectra of fully ^{15}N-labeled AAC−neomycin−CoASH (blue) and AAC−CoASH−neomycin (red) complexes. (b) AAC−neomycin−CoASH spectrum (blue) superimposed on the AAC−CoASH−neomycin spectrum (red) at identical contour levels after D_2O exposure for 25 h. Black arrows point to some resonances that have undergone solvent exchange faster in the AAC−neomycin−CoASH complex than in the AAC−CoASH−neomycin complex. (c and d) One-dimensional slice of the ^{1}H dimension located at 121.2 ppm in the nitrogen dimension (dotted line on the spectrum of panel b) from spectra of AAC−neomycin−CoASH (top) and AAC−CoASH−neomycin (bottom) complexes after D_2O exposure for 5 min (c) and 25 h (d). The dashed line is given as an eye reference based on a resonance at ∼9 ppm that is not affected by solvent.

opposite effects on T_m and R_H in the case of neomycin and paromomycin.

A decrease in the hydrodynamic radius indicates a more compact structure. Thus, the presented DLS data suggest that binding of CoASH to AAC leads to a more compact structure of the complex. A similar result, a decrease in the hydrodynamic radius in phosphoglycerate kinase (PGK) from 2.37 to 2.25 nm upon substrate binding, was obtained previously using small-angle neutron scattering.[34] However, the compactness of the ternary complexes depends on the way it is formed. When the coenzyme is bound first, the ternary complex has a more compact structure than when neomycin binds first. This agrees well with previous thermodynamic data showing that CoASH invokes a dramatic increase in antibiotic affinity as well as more favorable enthalpy and less favorable entropy of association of the antibiotic with AAC.[9] Association of neomycin with AAC prior to CoASH does not increase the affinity of CoASH for AAC; however, it reverses the enthalpic and entropic contributions, and contrary to what was observed in the binding of CoASH to AAC, the binding now becomes enthalpically favored and entropically disfavored. It appears that the bound neomycin changes the protein in such a way that it prevents the CoASH from having its stabilizing effect. The opposite behavior is observed for ternary complexes with paromomycin in which the pathway of the antibiotic first leads to a more compact structure. This suggests that the final AAC dynamic structure is dependent not only upon the pathway by which ligands associate with it but also upon the identity of the antibiotic. Differences in NOE patterns observed in NOESY-HSQC spectra lend further support to this notion and showed that dynamic properties of the protein backbone show significant differences between the two ternary complexes, confirming that indeed the dynamics of the protein in the ternary complex are dependent on how the complex is formed (i.e., the order of ligand addition).

Our earlier studies strongly suggested that solvent effects are manifested differentially between the different ternary complexes showing a strong dependence on the order of substrate addition.[24] In that work, binding enthalpies were determined in H_2O and D_2O. When the difference, $\Delta\Delta H$ ($\Delta H_{H_2O} - \Delta H_{D_2O}$), was plotted versus temperature, the ternary complexes of paromomycin and neomycin showed a similar dependence on temperature and yielded parallel lines. However, when the aminoglycoside was bound first, the ternary complexes showed differences similar to the differences in the behavior of their respective binary AAC−aminoglycoside complexes. In other words, binding of CoASH to the binary enzyme−aminoglycoside complex failed to overcome the effect of the aminoglycoside. [24] These results are consistent with the data presented in this work and highlight the extraordinary capability of AAC in recognizing similar substrates and the significance of protein dynamics in this process, which may be the key property for the high substrate promiscuity displayed by this enzyme.

The compactness of the ternary complexes and the influence of solvent also correlate well with the NMR data. Hydrogen−deuterium exchange data show that the AAC−CoASH−neomycin complex is more protected from solvent (red peaks of Figure 7a) than the AAC−neomycin−CoASH complex. The intensity of the peak at 6 ppm (Figure 7b,c) indicates complete proton exchange in the case of the AAC−neomycin−CoASH complex, while no significant exchange occurs in the case of the more compact AAC−CoASH−neomycin complex on the same time scale.

The clustering of peaks between 7.6 and 8.4 ppm observed in the [^{15}N]leucine spectrum of the AAC−neomycin−CoASH complex suggests that a region of AAC undergoes slow exchange between multiple conformations. Because this is not observed for the AAC−CoASH−neomycin complex, either the region is more dynamic in this complex and hence resonances move into an intermediary (and unobservable) exchange regime or the region is structurally well-defined and less dynamic. In either case, it is clear that there is a ternary pathway-dependent change in dynamics at the amino acid level. On the basis of the other data presented here, the latter situation of a relatively more well-defined structure of the AAC−CoASH−neomycin complex seems more likely.

Overall, the data from different methods agree that addition of neomycin first to AAC results in a ternary complex that is more dynamic than that seen after addition of CoASH first. In contrast, addition of paromomycin first to AAC results in a ternary complex that is less dynamic than that seen after addition of CoASH first. Though unique for each enzyme, ligand-dependent changes in dynamic properties of enzyme−aminoglycoside complexes and differential solvent effects are also observed with two other AGMEs.[33,35−38] However, the

dx.doi.org/10.1021/bi401635r | *Biochemistry* 2014, 53, 30−38

dependence of these properties on the order of substrate addition as observed for AAC is the first of its kind among AGMEs. In fact, we are not aware of any work describing any other system in which the order of ligand addition leads to significant differences in dynamic, structural, and thermodynamic properties of ternary complexes.

Understanding these molecular level intricacies of AGMEs that allow them to show various levels of substrate promiscuity while being able to discern between structurally very similar antibiotics may be relevant in future antibiotic design efforts. On a broader scale, however, this is an example of the dependence of dynamics on the order of complex formation in even the smallest complex that can have two pathways of formation (i.e., ternary). This observation inspires interest in such phenomena with higher-order complexes. Such dependence may also cause some of the observed "discrepancies" of data in the literature for the ternary complexes in different systems.

■ ASSOCIATED CONTENT

Supporting Information

Figures illustrating the effect of the order of addition on reaction kinetics, structures of neomycin and paromomycin, postulated structural positions of leucine residues, and DSC scans of binary and ternary complexes of the enzyme with two antibiotics and CoASH. This material is available free of charge via the Internet at http://pubs.acs.org.

■ AUTHOR INFORMATION

Corresponding Author

*Walters Life Sciences Bldg. M407, The University of Tennessee, Knoxville, TN 37996-0840. E-mail: serpersu@utk.edu. Telephone: (865) 974-2668. Fax: (865) 974-6306.

Author Contributions

A.L.N. designed and performed experiments, analyzed data, and wrote the paper. J.N. designed and performed the DLS experiments, analyzed DLS data, and wrote portions of the paper regarding DLS. E.H.S. designed experiments and supervised A.L.N. A.P.S. designed experiments, analyzed data, and supervised J.N.

Funding

This work is supported by a grant from the National Science Foundation (MCB-0842743 to E.H.S.). J.N. and A.P.S. thank the U.S. Department of Energy for financial support through the EPSCoR program (DOE-DE-FG02-08ER46528).

Notes

The authors declare no competing financial interest.

■ ACKNOWLEDGMENTS

We thank Dr. Kisliuk for help with DLS measurements, Dr. Liguo Song for mass spectroscopy analysis, and Dr. Edward Wright for help with AUC experiments.

■ REFERENCES

(1) Umezawa, H. (1974) Biochemical mechanism of resistance to aminoglycosidic antibiotics. *Adv. Carbohydr. Chem. Biochem. 30*, 183−225.

(2) Davies, J. E. (1991) Aminoglycoside-Aminocyclitol Antibiotics and Their Modifying Enzymes. In *Antibiotics in Laboratory Medicine* (Lorian, V., Ed.) 4th ed., p 1283, Lippincott Williams & Wilkins, Philadelphia.

(3) Shaw, K. J., Rather, P. N., Hare, R. S., and Miller, G. H. (1993) Molecular Genetics of Aminoglycoside Resistance Genes and Familial Relationships of the Aminoglycoside-Modifying Enzymes. *Microbiol. Rev. 57*, 138−163.

(4) Moazed, D., and Noller, H. F. (1987) Interaction of antibiotics with functional sites in 16 S ribosomal RNA. *Nature 327*, 389−394.

(5) Spotts, C. R., and Stanier, R. Y. (1961) Mechanism of Streptomycin Action on Bacteria: Unitary Hypothesis. *Nature 192*, 633−637.

(6) Davies, J. E. (1994) Inactivation of antibiotics and the dissemination of resistance genes. *Science 264*, 375−382.

(7) Wright, G. D. (1999) Aminoglycoside-modifying enzymes. *Curr. Opin. Microbiol. 2*, 499−503.

(8) Azucena, E., and Mobashery, S. (2001) Aminoglycoside-modifying enzymes: Mechanisms of catalytic processes and inhibition. *Drug Resist. Updates 4*, 106−117.

(9) Norris, A. L., Ozen, C., and Serpersu, E. H. (2010) Thermodynamics and Kinetics of Association of Antibiotics with the Aminoglycoside Acetyltransferase (3)-IIIb, a Resistance-Causing Enzyme. *Biochemistry 49*, 4027−4035.

(10) Norris, A. L., and Serpersu, E. H. (2010) Interactions of Coenzyme A with the Aminoglycoside Acetyltransferase (3)-IIIb and Thermodynamics of a Ternary System. *Biochemistry 49*, 4036−4042.

(11) Kay, L. E., Keifer, P., and Saarinen, T. (1992) Pure Absorption Gradient Enhanced Heteronuclear Single Quantum Correlation Spectroscopy with Improved Sensitivity. *J. Am. Chem. Soc. 114*, 10663−10665.

(12) Weigelt, J. (1998) Single scan, sensitivity- and gradient-enhanced TROSY for multidimensional NMR experiments. *J. Am. Chem. Soc. 120*, 10778−10779.

(13) Lin, D. H., Sze, K. H., Cui, Y. F., and Zhu, G. (2002) Clean SEA-HSQC: A method to map solvent exposed amides in large non-deuterated proteins with gradient-enhanced HSQC. *J. Biomol. NMR 23*, 317−322.

(14) Pellecchia, M., Meininger, D., Shen, A. L., Jack, R., Kasper, C. B., and Sem, D. S. (2001) SEA-TROSY (Solvent exposed amides with TROSY): A method to resolve the problem of spectral overlap in very large proteins. *J. Am. Chem. Soc. 123*, 4633−4634.

(15) Zhang, O. W., Kay, L. E., Olivier, J. P., and Formankay, J. D. (1994) Backbone H-1 and N-15 Resonance Assignments of the N-Terminal Sh3 Domain of Drk in Folded and Unfolded States Using Enhanced-Sensitivity Pulsed-Field Gradient NMR Techniques. *J. Biomol. NMR 4*, 845−858.

(16) Delaglio, F., Grzesiek, S., Vuister, G. W., Zhu, G., Pfeifer, J., and Bax, A. (1995) Nmrpipe: A Multidimensional Spectral Processing System Based on Unix Pipes. *J. Biomol. NMR 6*, 277−293.

(17) Johnson, B. A., and Blevins, R. A. (1994) Nmr View: A Computer-Program for the Visualization and Analysis of NMR Data. *J. Biomol. NMR 4*, 603−614.

(18) Freire, E., Vanosdol, W. W., Mayorga, O. L., and Sanchezruiz, J. M. (1990) Calorimetrically Determined Dynamics of Complex Unfolding Transitions in Proteins. *Annu. Rev. Biophys. Bioeng. 19*, 159−188.

(19) Sanchez-Ruiz, J. M. (1992) Theoretical analysis of Lumry-Eyring models in differential scanning calorimetry. *Biophys. J. 61*, 921−935.

(20) Schuck, P. (2000) Size-distribution analysis of macromolecules by sedimentation velocity ultracentrifugation and Lamm equation modeling. *Biophys. J. 78*, 1606−1619.

(21) Schuck, P. (2003) On the analysis of protein self-association by sedimentation velocity analytical ultracentrifugation. *Anal. Biochem. 320*, 104−124.

(22) Gun'ko, V. M., Klyueva, A. V., Levchuk, Y. N., and Leboda, R. (2003) Photon correlation spectroscopy investigations of proteins. *Adv. Colloid Interface Sci. 105*, 201−328.

(23) Daniel, W. W. (2009) *Biostatistics, a foundation for analysis in the health sciences*, Wiley, New York.

(24) Hu, X. H., Norris, A. L., Baudry, J., and Serpersu, E. H. (2011) Coenzyme A Binding to the Aminoglycoside Acetyltransferase (3)-IIIb Increases Conformational Sampling of Antibiotic Binding Site. *Biochemistry 50*, 10559−10565.

(25) Chervenak, M. C., and Toone, E. J. (1994) A Direct Measure of the Contribution of Solvent Reorganization to the Enthalpy of Ligand Binding. *J. Am. Chem. Soc. 116*, 10533−10539.
(26) Kresheck, G. C., Schneide, H., and Scheraga, H. A. (1965) Effect of D_2O on Thermal Stability of Proteins. Thermodynamic Parameters for Transfer of Model Compounds from H_2O to D_2O. *J. Phys. Chem. 69*, 3132.
(27) Sturtevant, J. M. (1977) Heat-Capacity and Entropy Changes in Processes Involving Proteins. *Proc. Natl. Acad. Sci. U.S.A. 74*, 2236−2240.
(28) Makhatadze, G. I., Clore, G. M., and Gronenborn, A. M. (1995) Solvent Isotope Effect and Protein Stability. *Nat. Struct. Biol. 2*, 852−855.
(29) Baldwin, R. L. (2010) Desolvation Penalty for Burying Hydrogen-Bonded Peptide Groups in Protein Folding. *J. Phys. Chem. B 114*, 16223−16227.
(30) Cooper, A. (2005) Heat capacity effects in protein folding and ligand binding: A re-evaluation of the role of water in biomolecular thermodynamics. *Biophys. Chem. 115*, 89−97.
(31) Burkhalter, N. F., Dimick, S. M., and Toone, E. J. (2000) Protein-Carbohydrate interaction: Fundamental considerations. In *Carbohydtrates in Chemistry and Biology* (Ernst, B., Hart, G. W., and Sinaý, P., Eds.) pp 863−914, Wiley-VCH, New York.
(32) Norris, A. L., and Serpersu, E. H. (2011) Antibiotic Selection by the Promiscuous Aminoglycoside Acetyltransferase-(3)-IIIb Is Thermodynamically Achieved through the Control of Solvent Rearrangement. *Biochemistry 50*, 9309−9317.
(33) Ozen, C., Norris, A. L., Land, M. L., Tjioe, E., and Serpersu, E. H. (2008) Detection of specific solvent rearrangement regions of an enzyme: NMR and ITC studies with aminoglycoside phosphotransferase(3′)-IIIa. *Biochemistry 47*, 40−49.
(34) Inoue, R., Biehl, R., Rosenkranz, T., Fitter, J., Monkenbusch, M., Radulescu, A., Farago, B., and Richter, D. (2010) Large Domain Fluctuations on 50-ns Timescale Enable Catalytic Activity in Phosphoglycerate Kinase. *Biophys. J. 99*, 2309−2317.
(35) Ozen, C., Malek, J. M., and Serpersu, E. H. (2006) Dissection of aminoglycoside-enzyme interactions: A calorimetric and NMR study of neomycin B binding to the aminoglycoside phosphotransferase(3′)-IIIa. *J. Am. Chem. Soc. 128*, 15248−15254.
(36) Ozen, C., and Serpersu, E. H. (2004) Thermodynamics of aminoglycoside binding to aminoglycoside-3′-phosphotransferase IIIa studied by isothermal titration calorimetry. *Biochemistry 43*, 14667−14675.
(37) Wright, E., and Serpersu, E. H. (2006) Molecular determinants of affinity for aminoglycoside binding to the aminoglycoside nucleotidyltransferase(2″)-Ia. *Biochemistry 45*, 10243−10250.
(38) Wright, E., and Serpersu, E. H. (2005) Enzyme-substrate interactions with an antibiotic resistance enzyme: Aminoglycoside nucleotidyltransferase(2″)-Ia characterized by kinetic and thermodynamic methods. *Biochemistry 44*, 11581−11591.